Vol. 16, No. 96, Jun., 1973

532.542 : 532.55

Studies on the Hydraulic Loss in Pipe Bends*

(Results for 90°-Screw Type Elbows)

By Mitukiyo MURAKAMI** and Yukimaru SHIMIZU***

A knowledge of hydraulic losses and secondary flows caused by elbows in a pipe line is of great importance in the field of hydraulic engineering.

The results with a single 90°-elbow and two 90°-elbows were published in the previous report, but from these results only, the hydraulic loss and the flow pattern due to three elbows or more, located successively in a pipe line, cannot be predicted perfectly.

By using various combinations of three 90°-elbows, the relationship between the hydraulic loss and the secondary flow is investigated. The loss and the flow pattern are strongly governed by the geometrical configuration of the pipe when the distance between the neighbouring elbows is small.

A comparison of this with the previous results gives an approach to estimate the secondary flow and the hydraulic loss which are caused by four elbows or more.

1. Introduction

A pipe line of a fluid machine or other hydraulic plants has often many complicated curved portions. When two or three bends are closely located in different planes, the water flowing through them acquires a strong spiral component of velocity. The bend loss and the secondary flow in curved ducts with two commercial elbows are discussed in the previous paper[1]. The use of curved ducts with three or more elbows is not uncommon in engineering practice. Itō[2] and also C. S. Lee[3] studied hydraulic losses of curved ducts with special combinations of three or more bends. With only these data, however, general feature of hydraulic losses and flow patterns can not be assessed.

In this paper, the relationship between the hydraulic loss and the velocity distribution in ducts with three or more 90°-elbows located successively is investigated experimentally. The results are compared with those in the previous paper and discussing is made on an approach to estimate the hydraulic loss due to many elbows combined.

2. Nomenclature

d: diameter of pipe

g: acceleration of gravity

H: total loss of head in gauge length

L_d: distance of downstream tap from the exit of the last elbow

L_{m1}: length of spacer between the first and the second elbows

L_{m2}: length of spacer between the second and the third elbows

L_u: distance of upstream pressure tap from the entrance of the first elbow, $=5d$

L: gauge length, $=L_d+\sum_{i=1}^{n} L_{mi}+L_u$

r: radial distance

R: radius of pipe, $=d/2$

p_1: static pressure at the first section located 5 times the pipe diameter from the entrance of the first elbow

p_2: static pressure at the second section located 300 times the pipe diameter downstream from the exit of the last elbow

p_s: wall pressure at any section downstream from the last elbow

R_e: Reynolds number, $=(V_m\ d)/\nu$

v_z: axial component of velocity

v_z': dimensionless axial velocity, $v_z'=v_z/V_m$

v_θ: tangential component of velocity

v_θ': dimensionless tangential velocity, $v_\theta'=v_\theta/v_m$

V_m: mean velocity calculated from orifice readings

γ: specific weight of water

ρ: density of water

* Received 8th October, 1970.

** Professor, Faculty of Engineering, Nagoya University.

*** Instructor, Faculty of Engineering, Nagoya University Chikusa-ku, Nagoya.

ζ_n: coefficient of total elbow loss as defined by Eq. (1) (suffix n in ζ expresses the number of elbows)

ζ_{ns}: coefficient of apparent total elbow loss calculated by Eq. (1) with p_s in place of p_2

λ: friction factor for straight pipe

ψ: angle of pipe line bent at the first and the second elbows, Fig. 2

ϕ: angle of pipe line bent at the second and the third elbows, Fig. 2

ν: kinematic viscosity

M: angular momentum flux

M': dimensionless expression of angular momentum flux

M_u': dimensionless expression of angular momentum flux through the section $1d$ upstream from elbow

M_d': dimensionless expression of angular momentum flux through a section downstream of elbow

M'': dimensionless expression of angular momentum flux of swirling created by uneven axial velocity at elbow entrance

$\bar{p}_u/\gamma$: dimensionless expression of mean pressure head measured at section $1d$ upstream from elbow entrance

$\bar{p}_d/\gamma$: dimensionless expression of mean pressure head measured at section $1d$ downstream from elbow exit

$\bar{v}_u^2/2g$: dimensionless expression of mean velocity head measured at section $1d$ upstream from elbow entrance

$\bar{v}_d^2/2g$: dimensionless expression of mean velocity head measured at section $1d$ downstream from elbow exit

3. Experimental apparatus and procedure

The general arrangement of the test apparatus is indicated in a schematic diagram, Fig. 1. A pipe line of 53.84 mm in diameter and with a hydraulically smooth surface was bent by three commercial 90°-elbows (JIS B 2301). The bent angles of the pipe line are defined in Fig. 2. Velocity distribution in a pipe section was measured along the diameters as shown in Fig. 3. The section was suitably selected according to flow conditions. Referring to the foregoing research, the length of spacers between elbows was selected as given in Table 1. The coefficient of total elbow loss included in the test length can be calculated by the following relation

$$H=(p_1-p_2)/\gamma=\lambda(L/d)(V_m^2/2g)+\zeta_n(V_m^2/2g) \quad (1)$$

and when three elbows are included, $\zeta_n=\zeta_3$.

Coupling depth of a screw joint between an elbow and a pipe has a considerable effect on the fitting loss of the elbow. Hence, the loss coefficient ζ_n will also be affected by the coupling depth of each elbow. When every joint between pipes and elbows was half screwed, ζ_n was reduced to 85 percent of

Table 1

L_{m1}/d, L_{m2}/d	0	1	3.55	7.1	10.1
ψ	0° ~ 180° (22.5° or 45°)				
ϕ	0°~180°~360° (22.5° or 45°)				

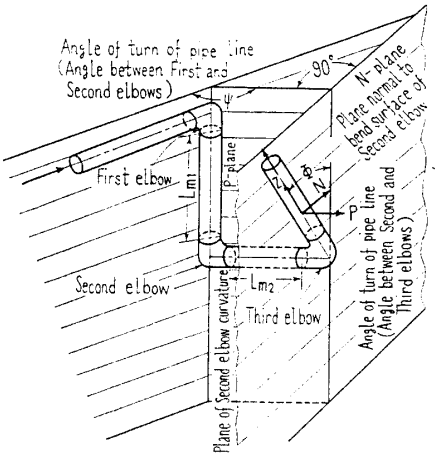

Fig. 2 Definition of angles of turn of pipe line

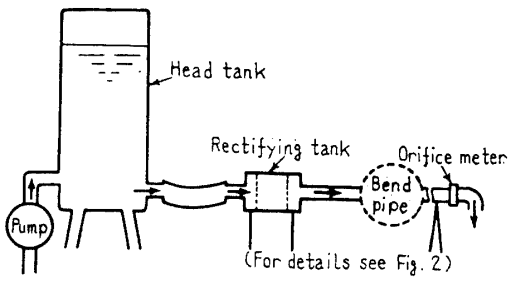

Fig. 1 Schematic diagram of test arrangement

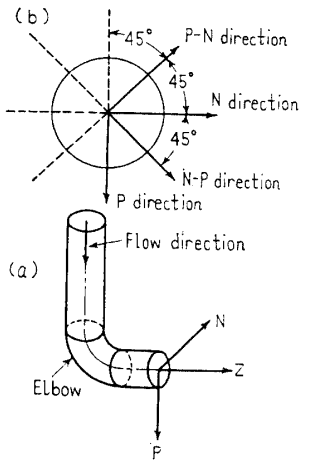

Fig. 3 Definition of P,N,NP and PN directions

the loss coefficient which would be obtained with a fully screwed joint. The percentage reduction was almost independent of the bent angles ψ and ϕ of the pipe line. Hereafter, the loss coefficient ζ_n is referred to the case when the pipe ends are fully screwed to the coupling parts. The experiments were performed within the range of Reynolds numbers from 10^4 to 2×10^5, where the change of ζ_n was less than ten percent. All of the results in this paper are referred to the case when the Reynolds number is about 10^5.

4. Experimental results and discussion

4·1 Bend loss and mutual interference of elbows

When the water flows through a pipe bent by two elbows located closely, distributions of velocity are much disturbed and the loss due to the two elbows combined is not equal to twice the loss of an elbow employed in an isolated condition. And when another elbow is located just downstream of the two elbows, the loss experienced in it will be much altered by the upstream conditions.

In order to discuss the losses due to many elbows located successively in a pipe line, an interference factor will be conveniently introduced.

Let the number of elbows situating in a pipe line be n, then an excess of loss due to the mutual interference of the elbows is given by

$$\Delta\zeta_n=\zeta_n-n\zeta_1 \quad \cdots\cdots(2)$$

If the number of elbows is reduced by one, the following relation will be obtained

$$\Delta\zeta_{n-1}=\zeta_{n-1}-(n-1)\zeta_1 \quad \cdots\cdots(3)$$

Divided by ζ_1, Eqs. (2) and (3) become, respectively,

$$I_n=\Delta\zeta_n/\zeta_1=\zeta_n/\zeta_1-n \quad \cdots\cdots(4)$$

$$I_{n-1}=\Delta\zeta_{n-1}/\zeta_1=\zeta_{n-1}/\zeta_1-(n-1) \quad \cdots\cdots(5)$$

From Eqs. (2) and (3)

$$\Delta\Delta\zeta_n\equiv\Delta\zeta_n-\Delta\zeta_{n-1}=(\zeta_n-\zeta_{n-1})-\zeta_1 \quad \cdots\cdots(6)$$

For the sake of simplicity, the difference given by Eq. (6) may be considered to be due to the loss experienced between the nth and the $(n-1)$th elbows. From Eq. (6) the following relation is obtained

$$\Delta I_n\equiv\Delta\Delta\zeta_n/\zeta_1=(\Delta\zeta_n-\Delta\zeta_{n-1})/\zeta_1$$
$$=(\zeta_n-\zeta_{n-1})/\zeta_1-1 \quad \cdots\cdots(7)$$

The values of ΔI_3 for different combinations of three elbows are shown in Fig. 4, where ΔI_2 is also plotted. In the combination of three elbows, when upstream two elbows are located in a U-shaped configuration, namely, when $\psi=0°$, ΔI_3 is almost independent of ϕ. In this case the loss in the third elbow is smaller than that experienced in an elbow isolated. ΔI_3 is increased by an increase of ϕ, which means an increse of the loss between the second and the third elbows, When $\psi\geqq90°$, the value of ΔI_3 is largely changed by the angle ϕ and the loss experienced between the second and the third elbows reaches the peaks at $\phi=135°$ and 225°, when $\psi=180°$. Figs. 5(a)~(c) show the effects of ψ and ϕ on the elbow loss for various spacers. The regions of 3 or 4 times the value of ζ_1 are shaded with oblique lines. When $L_{m1}=L_{m2}=0$ and $\psi=180°$, ζ_3/ζ_1 takes a maximum value at $\phi=135°$ or 225°, and this is the greatest loss coefficient obtained in all combinations of three elbows. When $\psi=0°$ and $\phi=0°$ (or 360°), ζ_3/ζ_1 takes a minimum value of 2.15. The loss coefficient decreases as the bent angle ψ decreases from 180° to 0°. This change of loss will be described later in relation with velocity distributions. In Fig. 5(b), ζ_3/ζ_1 reaches a maximum at the same angular positions as in Fig. (a), namely, at $\psi=180°$ and $\phi=135°$ or $\phi=225°$. But the value is reduced considerably. In Fig. 5(c), the maximum value of ζ_3/ζ_1 is further reduced. When the spacer length is increased, the disturbed velocity distributions due to the bends undergo a continuous process of adjustment and the curves of ζ_3/ζ_1 flatten off over the whole range of ψ and ϕ. When the spacer length L_{m1} or L_{m2} exceeds $7d$ or $10d$, the flow conditions in each bend are nearly the same as if they were considered in isolation, and the loss coefficient ζ_3/ζ_1 is nearly constant over the whole range of ψ or ϕ. This result is confirmed by the previous[1] investigation and also Ito's research[2].

4·2 Velocity distributions and elbow loss

4·2·1 Strength of swirling velocity and centre of uneven flow

When two or more elbows are located closely in

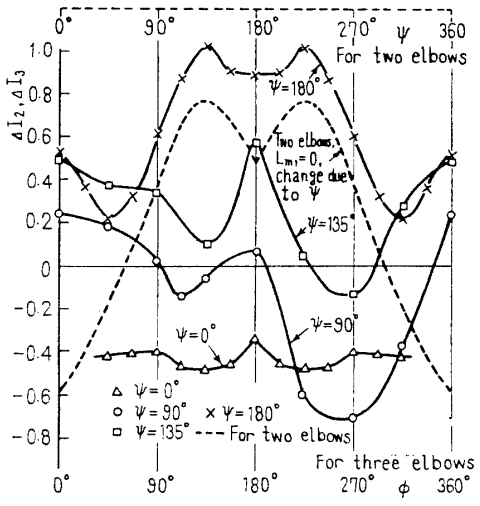

ΔI_2 : two elbows $L_{m1}=0$ (Broken line)
ΔI_3 : three elbows $L_{m1}=L_{m2}=0$ (Solid line)
Fig. 4 Values of ΔI_n

* The interference of elbows was expressed in a different way by Itō.

different planes, the velocity of the water leaving the elbows loses its uniformity and aquires a strong swirling component, which brings about a great hydraulic loss. As a measure of the strength of the swirling velocity, an angular momentum of water through a pipe section is considered as (Fig. 7)

$$M=\rho\int_0^{2\pi}\int_0^R v_z v_\theta r^2 dr d\theta \quad \cdots\cdots(8)$$

putting $r=Rr'$, $v_z=V_m v_z'$, and $v_\theta=V_m v_\theta'$ a dimensionless expression of Eq. (8) is obtained

$$M'=M/\rho V_m^2 R^3=\int_0^{2\pi}\int_0^1 v_z' v_\theta' r'^2 dr' d\theta \quad \cdots\cdots(9)$$

When two symmetrical vortices with opposite signs are formed in a section, as seen in the flow behind a simple bend, the vortices cancel each other and $M'=0$.

When the strengths of two vortices are not equal, a stronger vortex absorbs a weaker one in course of flow, and a single vortex is formed behind the section at which the symmetric vortices disappear. In this case an elevation of the wall pressure will be observed. To check the existence of this swirling motion, the wall pressure $p_{2=20d}$ at the section of $L_d=20d$ and p_2 at a section further downstream were measured. By subtracting these from a standared pressure p_1 measured at the section $5d$ upstream from the elbow entrance, the following expression can be derived.

$$S=\zeta_{n=3}-\zeta_{\substack{n=3\\ s=20d}}=\left(\frac{p_{2=20d}-p_2}{\gamma}\Big/\frac{V_m^2}{2g}\right)-\lambda\left(L_{2\to 20d}/d\right) \quad \cdots\cdots(10)$$

where $L_{2\to 20d}$ is the distance between two measuring sections of p_2 and $p_{2=20d}$.

When a secondary flow caused by a bend disappears before the section of $L_d=20d$, M_d' reduces to zero and $S=0$. As an example, the value of S and the angular momentum flux M_d' measured at the section $L_d=20d$ for various combinations of two elbows are compared in Fig. 6. Except in the neighbourhood of $\psi=0°$ and 180°, the curves of S and M_d' coincide fairly well, and S can be taken as a measure of the strength of a swirling flow. In Fig. 6, the loss coefficient is also plotted.

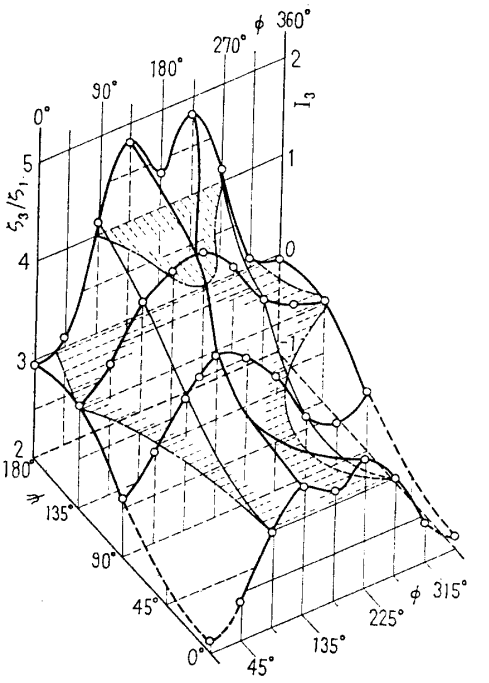

(a) $L_{m1}=L_{m2}=0$

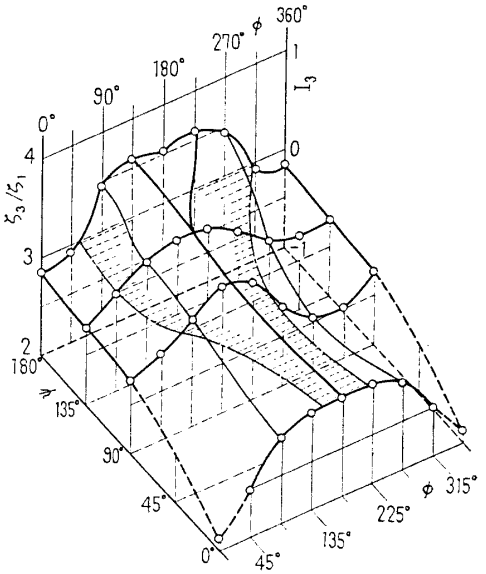

(b) $L_{m1}=L_{m2}=1d$

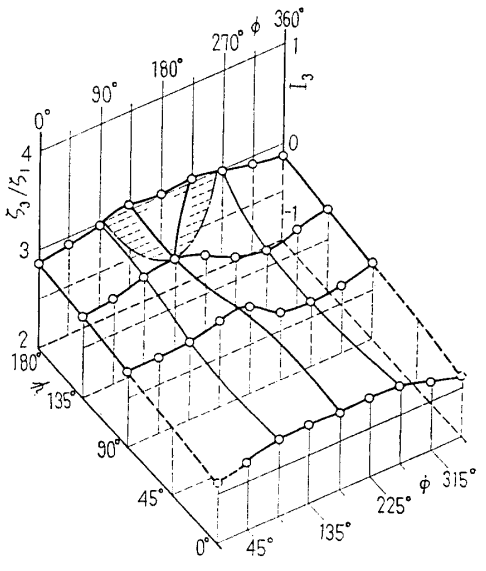

(c) $L_{m1}=L_{m2}=3.55d$

Fig. 5 Effects of bent angles ψ and ϕ on loss coefficient ζ_3/ζ_1 and interference coefficient I

When two elbows are closely located in a pipe line, the flow entering the downstream elbow will be greately disturbed. In order to define the centre of a velocity distribution, the following expressions for the moment of momentum of the flowing water are introduced

$$M_N=\rho\int_0^{2\pi}\int_0^R v_z v_z r_P r dr d\theta \quad \cdots\cdots(11)$$

$$M_P=\rho\int_0^{2\pi}\int_0^R v_z v_z r_N r dr d\theta \quad \cdots\cdots(12)$$

where M_N is the moment of momentum about the axis N-N and M_P is that about the axis P-P.

Making use of the relations

$$r=Rr',\quad r_N=r\cos\theta,\quad r=r_p\sin\theta,\quad v_z=V_m v_z' \quad \cdots\cdots(13)$$

Eqs. (11) and (12) become

$$M_N=\rho V_m^2 R^3\int_0^{2\pi}\int_0^1 v_z'^2 r'^2\sin\theta dr' d\theta \quad \cdots\cdots(11)'$$

$$M_P=\rho V_m R^3\int_0^{2\pi}\int_0^1 v_z'^2 r'^2\cos\theta dr' d\theta \quad \cdots\cdots(12)'$$

Let r_{0P} and r_{0N} be the distances of the deformed velocity centre from the axes of N-N and P-P respectively, then

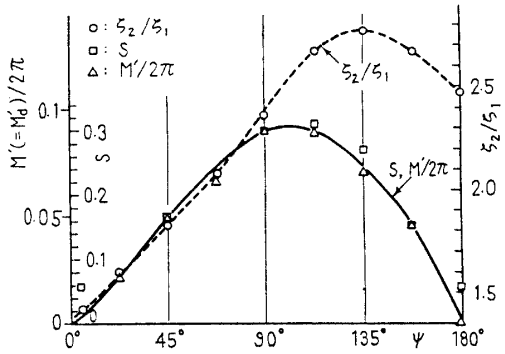

Fig. 6 Comparison of ζ_2/ζ_1, S and M' (at $L_d=20d$) for two elbows ($L_{m1}=0$)

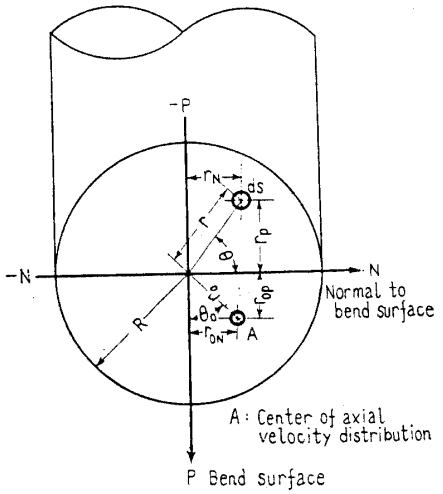

Fig. 7 Explanation of notation

$$M_N\equiv\rho\pi R^2 V_m V_m r_{0P}$$

$$M_P\equiv\rho\pi R^2 V_m V_m r_{0N}$$

These relations and Eqs. (11) and (12) give

$$r_{0P}/R=\frac{1}{\pi}\int_0^{2\pi}\int_0^1 v_z'^2 r'^2\sin\theta dr' d\theta \quad \cdots\cdots(14)$$

$$r_{0N}/R=\frac{1}{\pi}\int_0^{2\pi}\int_0^1 v_z'^2 r'^2\cos\theta dr' d\theta \quad \cdots\cdots(15)$$

When the radial distance of the centre A is denoted by r_0

$$(r_0/R)^2=(r_{0N}/R)^2+(r_{0P}/R)^2 \quad \cdots\cdots(16)$$

4·2·2 Velocity distributions

When a pipe line is turned three-dimensionally by two elbows, a swirling flow is generated after the bends, and the centre of flow velocity deviates from the pipe axis. The centre follows a helical path, and tends to approach the pipe axis in course of flow. When two elbows are located in the conditions of $L_{m1}=0$ and $\psi=90°$, a strong swirling motion is created. Distributions of axial velocities in this case are shown in Figs. 9(1)~(4). The angular momentum of the swirling water M_d' and the offset distance of the flow centre r_0/R measured at the

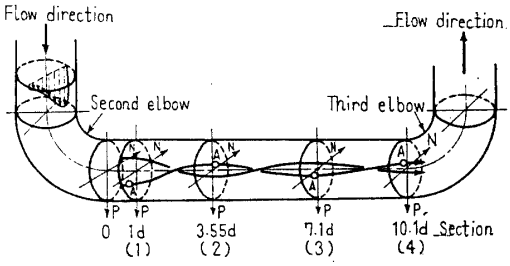

Fig. 8 Variation of eccentric center of flow velocity along pipe (downstream from second elbow, $\psi=90°$, $L_{m1}=0$)

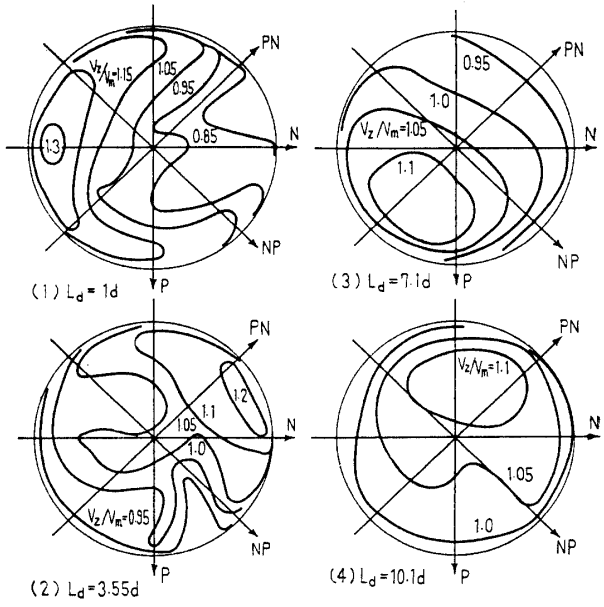

Fig. 9 Equi-axial velocity regions on sections downstream from second elbow ($\psi=90°$, $L_{m1}=0$)

section of $L_d=1d$ are shown against ψ in Fig. 10. When a pipe line is bent with $\psi=90°$ (or 270°), a strongest swirling motion occurs and the offset reduces to a minimum. A different relationship between ψ and M_d' or r_0/R is obtained for a different pipe section. Changes in the offset distance and its angular positions along the pipe, for $\psi=45°$ and 90°, are shown in Figs. 11(a) and (b). Here q is the angular displacement of the flow centre experienced in each pipe length of $L_d=1d$, and ω_0 expresses the initial angular position at the section $L_d=1d$ downstream from the elbow exit. The centre moves on a spiral path and at the section about $10d$ downstream from the elbow, r_0/R may be considered substantially to be zero. The relationship among q, ω_0, and ψ is shown in Fig. 12.

When the spacer length between the two bends is entirely eliminated, q and ω_0, respectively, take each maximum at $\psi\fallingdotseq 90°$ (270°), and become zero at $\psi=0°$ and 180°. This relation is changed in some extent by the spacer length. For various combinations of two elbows, Fig. 13 shows the change in the angular momentum flux of the swirling flow along the pipe. Different values of L_{m1} and ψ give different curves for M_d', but each curve changes parallel along the pipe. In Fig. 13, the value of M_d' for a combination of three elbows, where the strongest swirling motion is created, is also plotted.

With the knowledges described above, the inlet flow conditions of the third elbow located downstream of the two elbows can be assumed. When the water enters the third elbow with a deformed velocity distribution as in Fig. 14, a centrifugal force acting on the flowing water creates a secondary flow. To estimate the strength of the secondary flow, let the water be concentrated at the velocity centre A, then the centrifugal force has a moment arm of $(r_0/R)\sin\theta_0$ with respect to the centre line of the elbow. The angle θ_0 is found by the following equation with known values of q, ω_0, and

$$\theta_0=\pi+q\left(\frac{L_d}{d}-1\right)+\omega_0-\psi \quad \cdots\cdots(17)$$

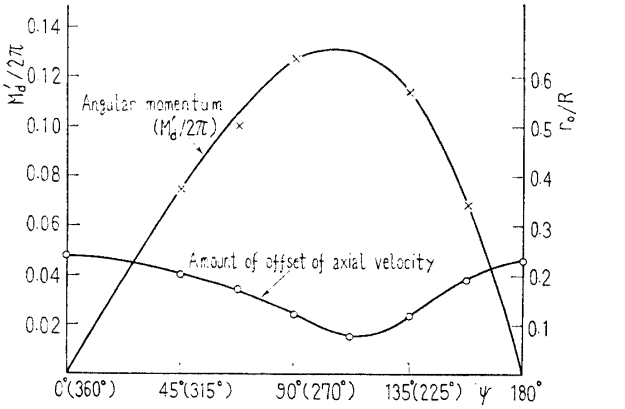

Fig. 10 M_d' and r_0/R measured at section $L_d=1d$ from second elbow (for two elbows, $L_{m1}=0$)

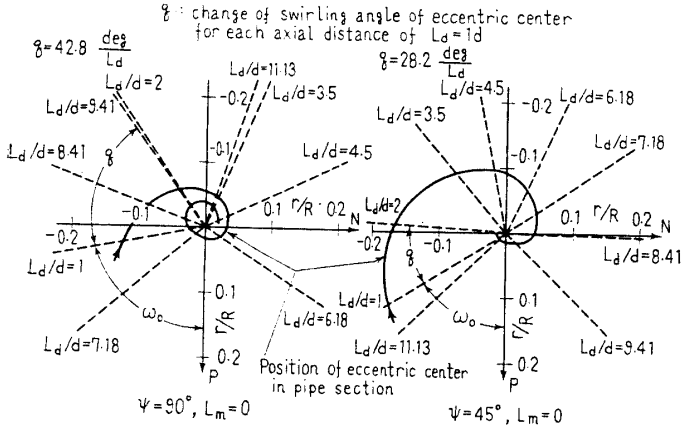

(a) Change of eccentric center along pipe center

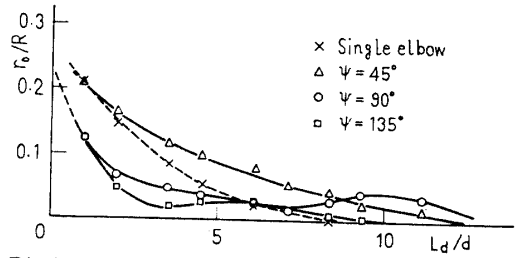

(b) Diminution of velocity distortion downstream from second elbow (for two elbows, $L_{m1}=0$)

Fig. 11

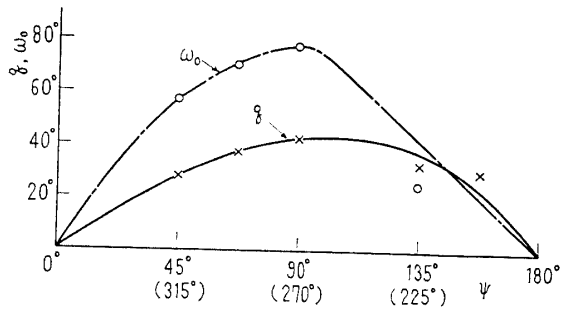

Fig. 12 The values q and ω_0 of swirling flow at exit of second elbow (two elbows, $L_{m1}=0$)

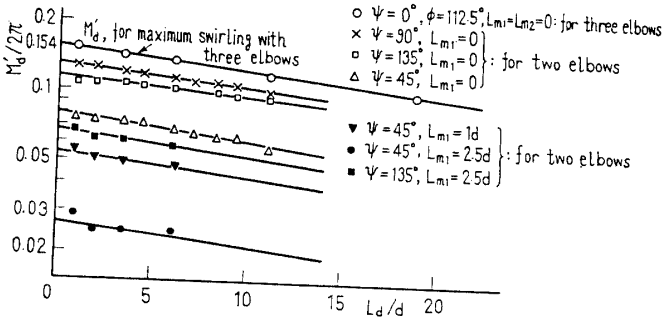

Fig. 13 Decay of swirling flow intensity behind second elbow

Thus, the angular momentum created by uneven inlet velocity distribution will roughly be given by

$$M''=\pi(r_0/R)(\sin\theta_0)m_z \quad \cdots\cdots(18)$$

The value of m_z in this equation is a dimensionless expression of the momentum flux of water and is given by

$$m_z=\rho\int_0^{2\pi}\int_0^R v_z^2 r dr d\theta/\rho\pi R^2 V_m^2$$

The value of m_z calculated for the most distorted flow is 1.13, and for a rough approximation m_z can be taken to be unity.

The swirling motion that develops before the elbow entrance is weakened when passing the curved path in the elbow and hence the angular momentum before the elbow M_u' will be reduced to $\alpha M_u'$ at the elbow exit. By combining this with the value given by Eq. (18), the angular momentum of the swirling flow at the third elbow exit is given by

$$M_d'=M''+\alpha M_u' \quad \cdots\cdots(19)$$

Now, the secondary flow at the exit of the third elbow is classified into the following three cases.

(1) $|M''|>\alpha|M_u'|$, namely, when the swirling flow caused by uneven velocity is predominant. This is a case when the second and the third elbows are closely located in a twisted-S form.

(2) $|M''|<\alpha|M_u'|$, namely, when the swirling motion continuing from the elbow upstream dominates the secondary flow downstream of the elbow. This is a case when the first and the second elbows are closely located in a twisted-S form and the third elbow situates comparatively apart from the second elbow.

(3) $|M''|\fallingdotseq\alpha|M_u'|$

An example of the case (1) is shown in Fig. 15. As is seen from Fig. 13, when $\psi=90°$ and 135°, a strong swirling component will be created downstream of the second elbow, neverthless, the sign of M_d', namely, the sign of swirling velocity downstream of the third elbow is changed by the setting angle of the third elbow, except in the cases of $L_{m1}=0$ and $L_{m2}\geqq 3.55d$ for $\psi=90°$, and $L_{m1}=0$ and $L_{m2}>1d$ for $\psi=$

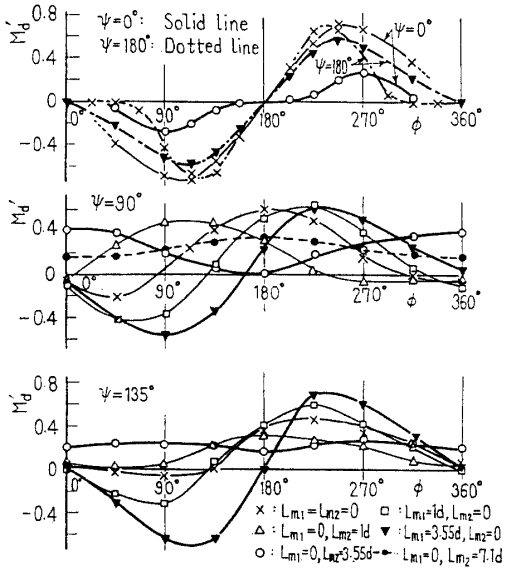

$M_d'>0$: clockwise swirling viewed from downstream
$M_d'<0$: counter-clockwise swirling viewed from downstream

Fig. 15 Strength of swirling flow (M_d') at section $L_d=20d$ downstream from third elbow

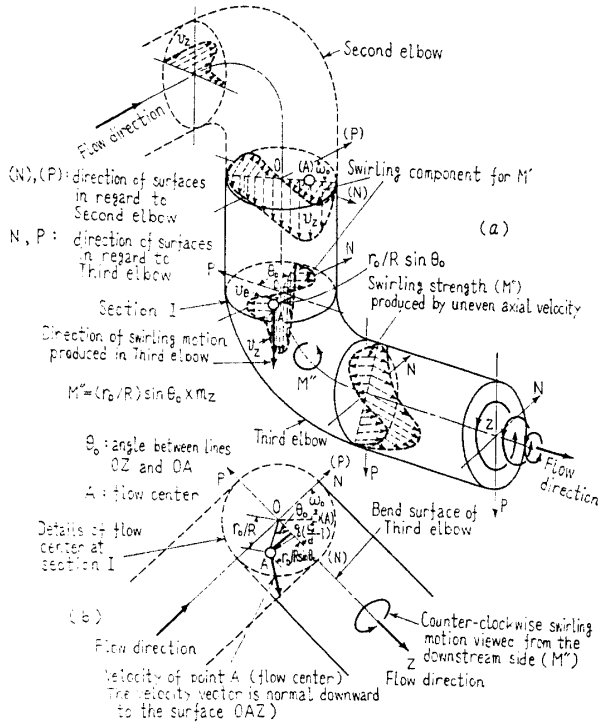

Fig. 14 Explanation of swirling motion (M'') produced by uneven axial velocity (r_0/R)

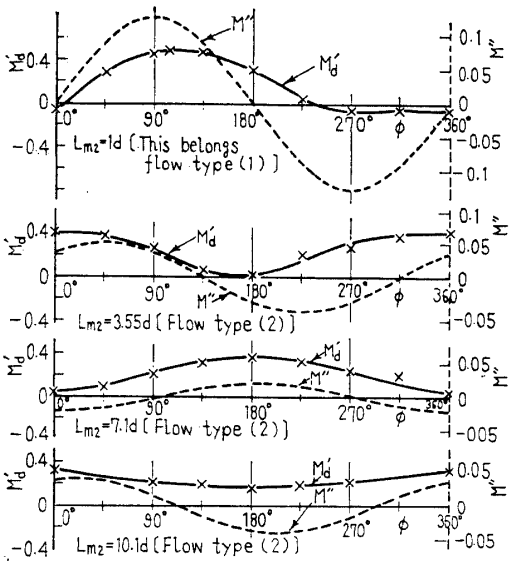

Fig. 16 Relation between M'' and M_d' (at the section $L_d=20d$ behind third elbow), ($\psi=90°$, $L_{m1}=0$) ($M_u'>0$)

135°, Fig. 15. When the first and the second elbows are located in a U-shaped or a S-shaped configuration in the same plane, the sign of M_d' changes at the angles $\phi=0°$ and 180°. The change of the spacer length alters the situation. When $L_{m1}=0$ and $\phi=0°$, and if L_{m2} is increased beyond $10d$, M_d' tends to zero and becomes independent of the angle ϕ. When $L_{m1}=0$ and $\phi=180°$, and if L_{m2} is increased over $5d$, M_d' also reduces substantially to zero.

An example of the case (2) is given in Fig. 16. The sign of the angular momentum flux downstream of the third elbow M_d' depends only on the sign of the swirling velocity or M_u' before the third elbow and the sign of M_d' is independent of the setting angle of the third elbow (except in the case $L_{m2}=1d$). When $L_{m1}=0$ and $\phi=90°$, this flow pattern will be observed beyond the range $L_{m2}/d=3.55$. If the angle ϕ is changed to 135°, the limiting condition for this flow is $L_{m2}/d=1$. In these cases deformation of velocity distributions is greatly reduced before the third elbow, and the swirling motion caused by this deformed velocity distribution is so small that it does not govern the sign of the swirling velocity behind the third elbow. For reference, the angular momentum flux M'' calculated by Eq. (18) is also plotted in Fig. 16. M'' changes its sign twice when ϕ is increased from zero to 360°. It is noticed that the curves of M_d' and M'' have a similar tendency. When the third elbow is located $10d$ or more downstream from the second elbow, the velocity profile before the third elbow is approximately axi-symmetric. If the flow has a swirling component, the third elbow causes a special hydraulic loss due to this axi-symmetric swirling flow. An example of this case is shown in Fig. 17, where M_u' denotes the angular momentum flux through the section $1d=L_u$ upstream from the elbow inlet and M_d' is that at the section $1d=L_d$ downstream from the elbow outlet. The swirling motion which will be observed in a pipe line having two or three elbows is shaded by oblique lines. The ratio M_d'/M_u' which is found by using this result will correspond to the coefficient α given in Eq. (19).

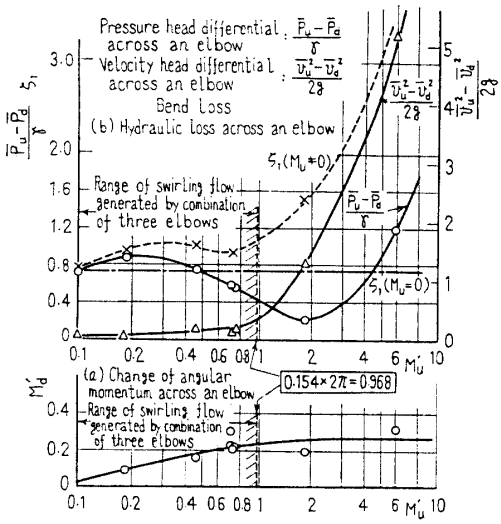

Fig. 17 Change of energy and angular momentum fluxes across an elbow in axi-symmetric swirling flow ($L_u=1d$, $L_d=1d$)

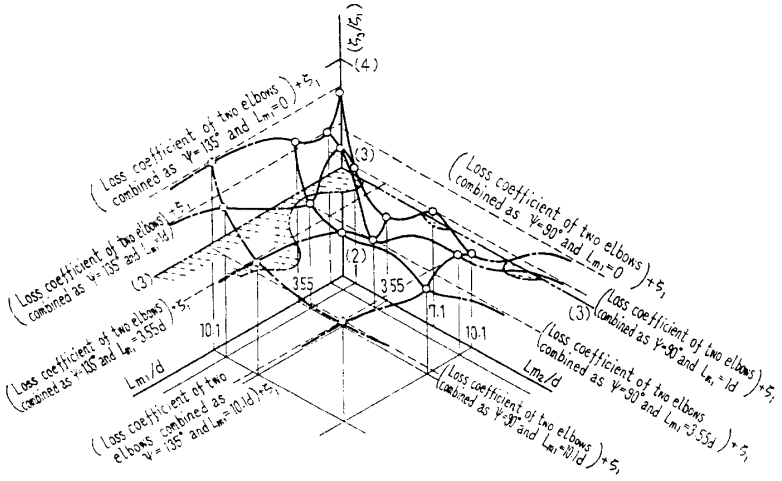

Fig. 18 Effects of spacer length on loss coefficients for three elbows combined as $\psi=90°$ and $\phi=135°$ [(flow type (2)]

The case (3), namely, when $|M''|=\alpha|M_u'|$, is possible theoretically, but it is confined to a special combination of three elbows and its experimental verification is very difficult.

The above results may be summarized as follows: When an angular momentum flux M_u' and the position of velocity centre r_0/R are known at the entrance of an elbow, the strength of the swirling component at its exit can be estimated by the following procedure.

(1) When the bent angle of the elbow θ_0 is decided, the moment arm is given by $(r_0/R)\sin\theta_0$, (Fig. 14), and the angular momentum flux M'' produced by the uneven velocity distribution can be calculated by Eq. (18).

(2) With the knowledges of the angular momentum flux at an elbow entrance M_u', the reduction of M_u' in the elbow can be found by use of Fig. 17(a), and the swirling strength at the elbow exit $\alpha M_u'$ is known.

(3) The sum of the above two, namely, $M''+\alpha M_u'$ gives the strength of swirling motion at the elbow exit.

4·2·3 Bend loss

In the flow in case (2), the loss due to elbows increases as the swirling velocity developed downstream of the third elbow increases. The loss coefficient ζ_3/ζ_1 of three elbows is shown in Fig. 18, when $\phi=90°$

and $\phi=135°$. When $L_{m1}=0$ and L_{m2} is increased from zero to $3.55d$, the value of ζ_3/ζ_1 decreases and shows a minimum at $L_{m2}=3.55d$, beyond which ζ_3/ζ_1 increases again. The second maximum occurs at $L_{m2}=7.1d$. When L_{m2} is increased further, ζ_3/ζ_1 follows a wavy path and tends to a constant value of $(\zeta_2+\zeta_1)/\zeta_1$. The value $(\zeta_2+\zeta_1)$ means $\phi=90°$ $\phi=90°$ the sum of the loss coefficients of two elbows combined as $L_{m1}=0$ and of an isolated elbow. Employing the third elbow at the sections (2), (3), and (4) in Fig. 8, respectively, under the condition of $\phi=135°$, the values of angular momentum flux M_d' and M'' are examined. The results are shown in Table 2. If the sign of M_u' before the third elbow coincides with that of M_d' occurring in the third elbow, the loss of the elbows combined is increased and vice versa.

As described already, when three elbows are combined as $L_{m1}=0$ and $L_{m2}\geqq 10d$, the axial velocity at the entrance of the third elbow is almost axi-symmetric. Figure 17(b) shows the loss experienced in the third elbow in this case. $(\bar{v}_u{}^2-\bar{v}_d{}^2)/2g$ and $(\bar{p}_u-\bar{p}_d)/\gamma$ are the differences in velocity and the pressure heads observed at the entrance and the exit of the elbow, respectively. $\zeta_1(M_u'=0)$ and $\zeta_1(M_u'\neq 0)$ denote the loss coefficients for the cases of $M_u'=0$ and $M_u'\neq 0$, respectively. Both $(\bar{v}_u{}^2-\bar{v}_d{}^2)/2g$ and ζ_1 increase rapidly as the swirling component, namely, M_u' increases. This fact is confirmed by the results in Fig. 17(a).

When the flow due to bends corresponds to the case (1) in section 4·2·2, the magnitude of the secondary flow behind the third elbow is not always a measure of the elbow loss. An example of this case is shown in Figs. 19(a) and (b). Though the strength of the secondary flow M_d' is low, a great loss coefficient is seen at about $\phi=135°$ or 90°, in the figure. To check the flow conditions, velocity distributions at the exit and the inlet sections of the

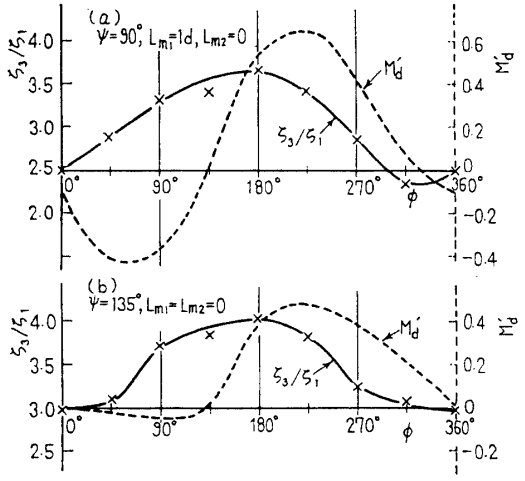

Fig. 19 Relation between bend loss and vortex strength [Type (1) flow, M_d' at $L_d/d=20$]

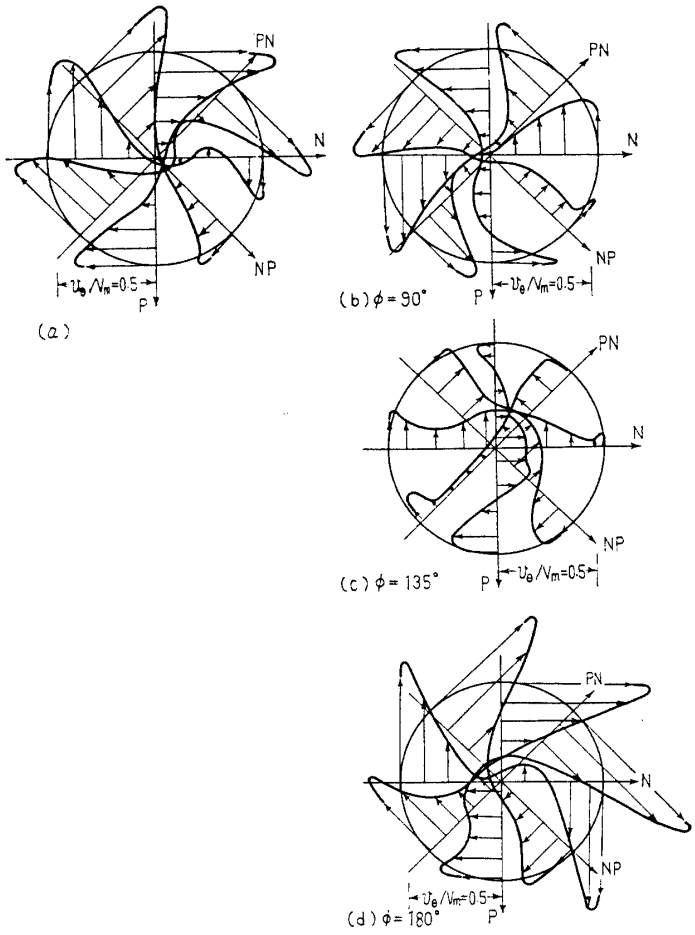

(a) : swirling velocity just before third elbow
(b)~(d) : swirling velocity at $L_d=1d$ behind third elbow

Fig. 20 Effects of bent angle ϕ on swirling flow direction behind third elbow (for $\psi=90°$, $L_{m1}=1d$ and $L_{m2}=0$)

Table 2

$L_{m2}/d+0.5d/d$	Direction of M_u' before an elbow	Direction of M	Swirling strength(M_d')	Bend loss
(1+0.5)	(Clockwise)	(Clockwise)	Large (0.48)	Large
3.55+0.5	Clockwise	Counter-clockwise	Small (0.08)	Small
7.1+0.5	Clockwise	Weak clockwise	Large (0.33)	Large
10.1+0.5	Clockwise	Counter-clockwise	Small (0.24)	Small

In the first column a short length $0.5d$ within an elbow is added

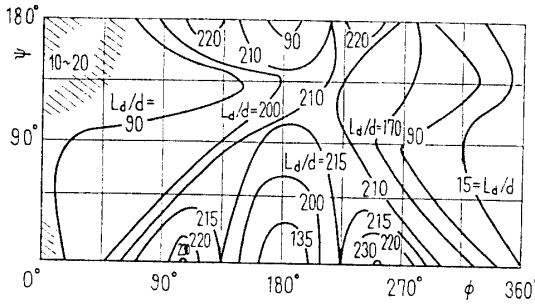

Fig. 21 Distance influenced by bends combined with three elbows ($L_{m1}=L_{m2}=0$)

third elbow were measured. The results for $\phi=90°$ are shown in Figs. 20(a)~(d). The direction of the swirling component behind the elbow is counter clockwise when $\phi=90°$ and clockwise when $\phi=180°$. The velocity distribution for $\phi=135°$ shows a transient stage. In this case M'' and $\alpha M_u'$ are nearly equal but have opposite signs, and the swirling velocity behind the third elbow will be largely reduced. The hydraulic loss in this case is remarkably increased and ζ_3/ζ_1 shows a high value.

4·2·3 Distance influenced by elbows

When elbows are closely located, the effects of the elbows extend far downstream. An example for $L_{m1}=L_{m2}=0$ is shown in Fig. 21. As described already, when the elbows are combined as $\phi=0°$ or $180°$ and $\phi=115°$ or $245°$, an intesive swirling is created downstream of the third elbow. The effects of the elbows in this case extend about 230 times the pipe diameter.

5. Conclusions

(1) When three elbows are located successively in a pipe line, the coefficient of the bend loss is altered in complicated way depending on bent angles of the pipe line and on the spacer length.

(2) The secondary flow developed by the bends in elbows was measured for various values of ψ, ϕ, L_{m1} and L_{m2} and the bend loss was discussed in relation to the secondary flow. An approach for the estimation of the secondary flow and the loss is also given.

References

(1) Murakami, M., et al., *Bull. JSME*, Vol. 12, No. 54 (1969-12), p. 1369.
(2) Itō, H, *Memo Inst. High Speed Mech., Tohoku Univ.*, Vol. 15, No. 142 (1959/1960), p. 37.
(3) Lee, C.S., *Gesundh Ingr*, Vol. 12, No. 89 (1968), p. 367.

Discussion

T. SHIRAISHI (Mitsubishi Heavy Industries, Ltd.)

(1) Suffix Z_u, N_u, and P_u for upstream and Z_d, N_d, and P_d for downstream of an elbow are used to identify the Z, N, and P components of a vector, respectively. On the basis of momentum theory, the angular momentum vectors of water upstream $\omega_u(=\omega_{Zu}+\omega_{Nu}+\omega_{Pu})$ and downstream $\omega_d(=\omega_{Zd}+\omega_{Nd}+\omega_{Pd})$ are connected with the moment T due to wall in the following way

$$\omega_u+T=\omega_d \quad \cdots\cdots(\text{i})$$

where

$$\left.\begin{aligned}&|\omega_Z|=M\\&|\omega_N|=M_N-\rho V_m\int_0^{2\pi}\int_0^R v_Z r_P dr d\theta\end{aligned}\right\}$$

and

$$\left.|\omega_P|=M_P-\rho V_m\int_0^{2\pi}\int_0^R v_Z r_N dr d\theta\right\} \quad \cdots\cdots(\text{ii})$$

and T_Z, T_N, and T_P denote the Z_u, N_u, and P_u components of T, respectively.

Considereing the control surfaces before and after the third elbow, the following relation is derived

$$|\omega_{Pu}|+|T_P|=|\omega_{Zd}| \quad \cdots\cdots(\text{iii})$$

Now, the angular momentum flux of water is given by

$$M''=\frac{M_{Pu}}{\rho V_m^2 R^3}mz \quad \cdots\cdots(\text{iv})$$

From Eqs. (ii)~(iv), the following relation is obtained

$$M_d'=\frac{M''}{mz}-\int_0^{2\pi}\int_0^R v_Z' r_N' r' dr' d\theta+\frac{|T_P|}{\rho V_m^2 R^3} \quad \cdots\cdots(\text{v})$$

From this relation it is clear that the assumption made on Eq. (19) is not reasonable, though the expression of Eq. (v) includes the term M''.

(2) When many elbows are employed in a pipe line, do the upstream $(n-m)$ elbows affect the flow in the nth elbow downstream of them?

(3) Is the same rate of change in bend loss due to the coupling depth variation expected if the number of elbows is increased from 2 to 3?

H. ITŌ (Tōhoku University):

(4) The discusser is of opinion that although the authors' results were obtained with 2 in. commercial screw elbows, the hydraulic performance of screw elbows having sudden enlargement and contraction of section will be greatly different from that of flanged elbows with the internal diameter equal to that of the straight pipe(*1). As an example, the bend loss coefficient measured at various distances down-

(*1) Itō, H. and Imai, K., *Jour. Japan Soc. Mech. Engrs.* (in Japanese), Vol. 69, No. 568 (1967-5), p. 560.

stream from the exit of a single 90° bend in a pipe line is shown in Append.-Fig. 1(*2), where ζ_t is the gross bend loss coefficient, namely, the value of ζ measured at the piezometer station placed far downstream from the bend. [In the figure, elbow means the $1^1/_4$ in. commercial screw elbow of Japanese industrial specification, R is the radius of center line of bend and $a(=d/2)$ the internal diameter of bend.] The figure shows that the screw elbow has less effect on the flow downstream from the elbow, at least with respect to the head loss. Because the relative amount of the enlargement and the contraction of section is different depending on the elbow size, an elbow of a different nominal size will give rise to a quantitative difference in the head loss.

(5) As the discusser has mentioned in the discussion in another paper published by one of the authors, Howthorne(*3) and Horlock(*4) have investigated theoretically the secondary flow in bends, the results of which will be useful for the authors' study. For instance, how did the authors treat the effects of the centrifugal force resulting from the curved passage? The discusser cannot understand it.

Authors' closure

The authors wish to thank the discussers for their interesting and valuable comments on this paper:

(1) We agree that Eq. (19) is not a resonable expression for a swirling flow intensity across an elbow. But the flow in the elbow is very complicated in nature and an expression for the moment of wall friction is hard to obtain. We paid attention to measurable quantities, namely, the offset amount of the flow r_0/R and the angular momentum flux M'' before an elbow, and tried to find the intensity of a swirling motion behind the elbow. The results obtained in this way were verified by the experiments.

(2) The problem is being investigated at present and we have no affirmative reply. But the value of m is assumed to be 4 or 5 from the results given in the Append.-Fig. 2, where all of the spacer length separating elbows are eliminated. The intensity of the swirling motion due to elbow bends increases with n, the number of elbows, but it is saturated at about $n=4$ or 5. In this case the value of the total loss coefficient ζ_n divided by $n\zeta_1$, namely, the mean value of the coefficient per one elbow, becomes smaller than 1, the loss coefficient of an isolated elbow.

(3) The effects of the screw depth on the bend loss are not altered by the number of elbows n. The loss coefficient ζ_n is altered at the same rate by change of the coupling screw depth, when n is increased from 2 to 3. The loss in half screwed elbows is lowered to 85 percent of the loss in fully screwed elbows.

(4) The value of the loss coefficient is altered, as you indicated, somewhat by the elbow size. Even with the same size of elbows, a little difference in the elbow loss is experienced, which will probably be attributable to the difference in the enlargement or the contraction of the water way in the elbows. In this respect, a further research will be needed for practical purpose.

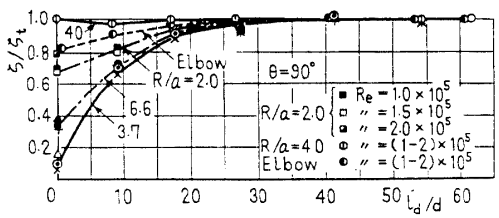

Append.-Fig. 1

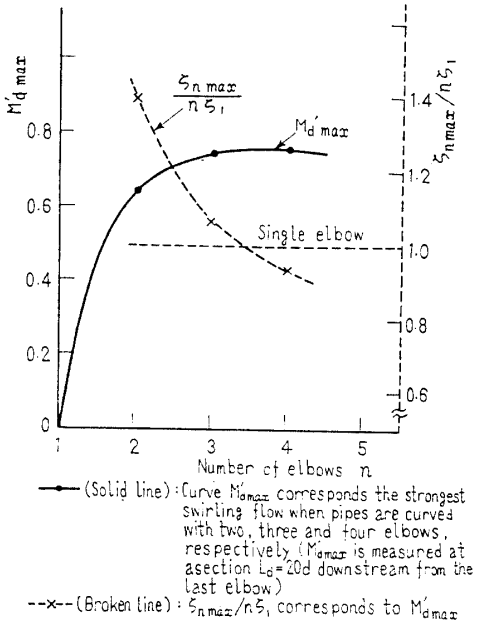

Append.-Fig. 2

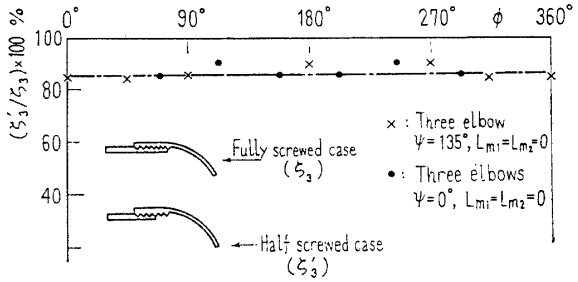

Append.-Fig. 3 Effects of coupling depth on loss coefficients in screw elbows

(*2) Itō, H., *Trans. ASME*, Ser. D, Vol. 82, No. 1 (1960-3), p. 131.
(*3) Hawthorne, W.R., *Proc. Roy. Soc. Lond.*, Ser. A, Vol. 206, No. 1086 (1951-5), p. 374.
(*4) Horlock, J.H., *Proc. Roy. Soc. Lond.*, Ser. A, Vol. 234, No. 1198 (1956-2), p. 335.

(5) The internal flow in an elbow as employed in this test is too complicated for theoretical treatment. We intended, as the first step, an experimental study on the flow pattern and we tried to find the intensity of the swirling flow behind an elbow, with knowledges of the offset amount r_0/R and the angular momentum flux before the elbow. In the second step a theoretical consideration will be needed.

Errata (Vol. 16, No. 94, April, 1973)

Author	Page	Column	Line	For	Read
H. SAITO et al.	712	left	38	$\sin(j\pi x/l)xq(t)$	$\sin(j\pi x/l)q(t)$
S. TAKAHASHI et al.	722	right	4 (Discussion)	moment o inertia	moment of inertia
S. NAMIE	755		Eq. (14)	Σ	$\sum_{\mu}$
	760	left	32	$\bar{A}$	A
T. AIDA et al.	771	right	34	σ/dr	δ/dr
	772	right	4	cases	case
	774	right	7	φ_{BA}	σ_{BA}